Journal of Inclusion Phenomena and Molecular Recognition in Chemistry **32:** 311–329, 1998.

Strategy for Designing New Li^+ ion Specific Receptors. A Combination of Theoretical Calculations and Experimental Techniques

KENZI HORI*
Department of Applied Chemistry and Chemical Engineering, Faculty of Engineering, Yamaguchi University, Ube, 755-8611 Japan

HIROSHI TSUKUBE
Department of Chemistry, Graduate School of Science, Osaka City University, Osaka 558-8585, Japan

(Received: 14 August 1997; in final form: 22 September 1997)

Abstract. Our strategy for designing new receptor molecules specific for Li^+ ions is to combine two methods, theoretical calculations and the experimental technique. In developing the Li^+ ion-specific receptors, we regarded crown ether derivatives of a 12-membered ring and side arms with functional groups as building blocks. This strategy worked well to synthesize new receptor molecules which selectively bind and transport the Li^+ ion.

Key words: new Li^+ ion specific receptors, theoretical calculations, experimental techniques, aza-12-crown-4, sidearm.

1. Introduction

Macrocyclic compounds have been synthesized to obtain new molecules which mimic receptors of biological importance [1]. Some of them can selectively encapsulate and transport alkali metal ions in membrane systems. Many research groups have synthesized a variety of macrocyclic ether and amine derivatives and successfully applied them to catalysis, separation, detection, enzyme mimics and so on [2]. Macrocyclic rings are believed to have cavities suitable for binding a specific cation. In particular, special attention has been focused on 12-crown-4, 13-crown-4 and 14-crown-4 compounds as Li^+ ion-specific receptors [3]. The receptors of the small Li^+ ion are very important tools for analysis and separation in biological and environmental systems. Although the diameter of the Li^+ ion is formally size-fitted to the cavity of 12-crown-4, its derivatives generally exhibit selectivity for the Na^+ ion [4]. One reason is that they tend to form stable 2 : 1 complexes with the Na^+ ion and the other is that the Li^+ ion is too heavily solvated to be bound/extracted via

* Author for correspondence.

1 : 1 complexation with these crown compounds. Although the ion-hole relation is a very important factor determining ion selectivity, this is not the only factor that introduces the desired property.

We have synthesized and characterized some macrocyclic compounds with ion selectivity, especially for Li^+ ions [6]. Our experiment confirmed that aza-15-crown-5 ethers have no selectivity for the Li^+ ion. We can assume that crown rings with more than 5 donor atoms cannot construct holes suitable for the small Li^+ ion. As the stability of complexes can be controlled by the number of donor atoms in the crown derivatives, adding one or more side arms to mono or poly-aza-12-crown-4 rings is an alternative technique to get more donor atoms [7]. It was possible to construct new Li^+ ion-specific receptors by using aza-crown ethers and sidearms. Therefore, we can regard crown rings and side arms as building blocks to construct new Li^+ ion-specific receptors. Our choice of basic building blocks are 9–12 membered rings with three or four donor atoms as shown in Figure 1. The 12-membered ring is considered to have a hole in which the Li^+ ion easily fits. Additional blocks are side arms with a nitrogen or an oxygen donor. The combination of basic and additional blocks produces a variety of crown ethers with one or more side arms.

Although there are many useful building blocks and their combinations, it takes a long time to synthesize and assess whether or not new compounds show a selectivity for the Li^+ ion. We want to know which combination is expected to have the most desired property, that is, the selective binding and transport of Li^+ions. In order to construct macrocyclic compounds with Li^+ ion selectivity, we have to know which blocks and crown derivatives closely relate to the function before synthesizing and characterizing them. The information we need is (1) the hole size of a crown ring and (2) the stabilization energy accompanied by complex formation. Theoretical calculations make it possible to calculate these two factors. Moreover, they are also useful in explaining the origin of functions displayed by crown compounds. Molecular orbital (MO) [8] and density functional calculations [9], molecular mechanics [10], molecular dynamic calculations [11], and Monte Carlo simulations [12] have been used for characterizing the properties of the crown compounds.

There should exist some systematic methods to predict whether or not new molecules show desired functions which, in the present case, are selective binding and transporting of Li^+ ions. It is this combination of theoretical calculations and experimental techniques that works not only for obtaining some guiding principles but for explaining experimental results. In the present paper, we will show how we have been using these two methods to design and characterize a new series of macrocyclic receptors which selectively bind and transport the Li^+ ion.

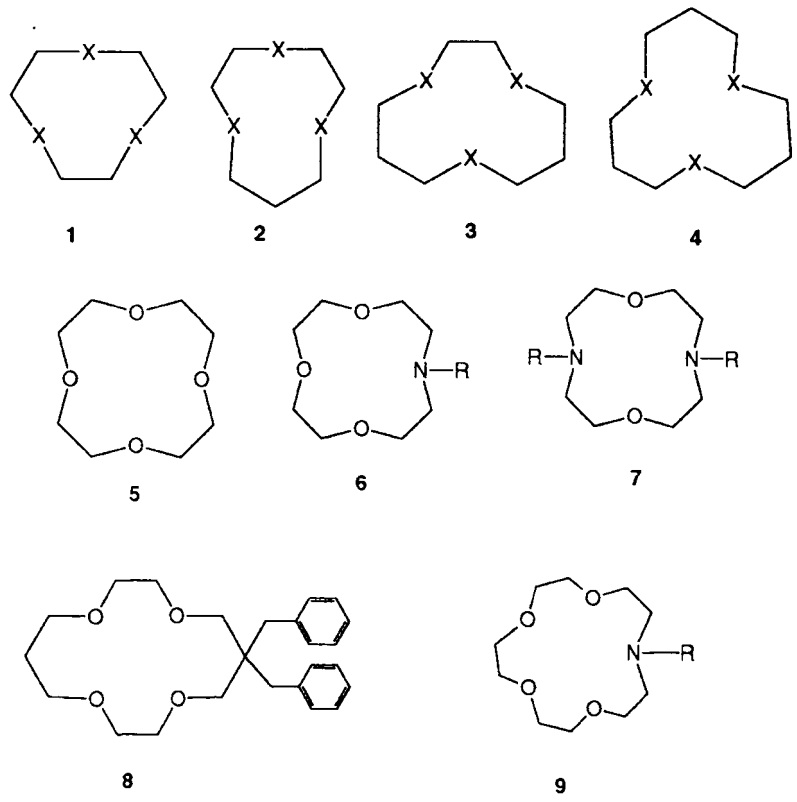

Figure 1. Geometries of crown ethers and related materials as building blocks.

2. Design of New Macrocyclic Compounds Using MO Calculations

2.1. THE HOLE SIZE OF THE CROWN RING

The basic blocks are crown rings with several donor atoms which can coordinate with metal ions [13]. First of all, the hole size of the crown ring was examined since this is one of the most important factors determining the ion selectivity. When we quantitatively deal with the hole size of a macrocyclic ring, we have to calculate the size in a systematic manner. For a crown compound with three donor atoms (X), we defined its hole size as the radius (r) of the circle consisting of three donor atoms (Drawing 1). The sphere center of the donor atoms was estimated by the least

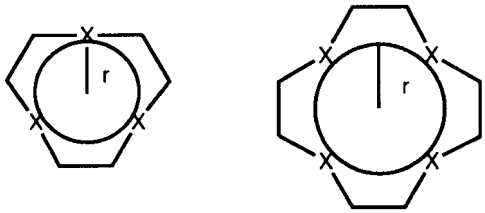

Drawing 1.

Table I. Free-X, Comp-X radii, Δr^*_{FC} and Li-X lengths in Å unit calculated for *n*-crown-X_3 and their Li^+ complexes by the MNDO calculations

	Free-O	Comp-O	Δr_{FC}	Li-O		Free-N	Comp-N	Δr_{FC}	Li-N
9-crown-O_3	1.661	1.541	0.120	2.153	9-crown-N_3	1.718	1.711	0.007	2.157
10-crown-O_3	1.707	1.643	0.064	2.187	10-crown-N_3	1.871	1.759	0.112	2.168
11-crown-O_3	1.729	1.691	0.038	2.083	11-crown-N_3	1.989	1.795	0.194	2.132
12-crown-O_3	1.790	1.772	0.018	2.084	12-crown-N_3	2.059	1.865	0.194	2.120

* Δr_{FC} is the difference between the Free-X and Comp-X radii.

squares fitting for crown rings with more than four donor atoms. We calculated the mean length between the center and each donor atom and defined that length as the hole size of the crown ring.

It is possible to calculate the two radii, one for a free crown molecule and the other for the crown molecule in a complex. We call them the Free-X and the Comp-X radius (X = O or N), respectively. We calculated these radii of *n*-crown-X_3 (**1**–**4**) and 12-crown-O_4 (**5**) in order to be certain that this method would be useful for the estimation of hole sizes of crown compounds. The MNDO hamiltonian in the MOPAC Ver. 5 [14] was adopted for geometry optimization of free crown ethers and their Li^+ complexes. Figure 2 shows that the calculated hole sizes correlate well with the number of atoms in the crown rings. In the range of n = 9 to 12, the Free-O line stays lower than the Free-N line. For example, the Free-N radius of 10-crown-N_3 (**2N**) is 1.871 Å and the Free-O radius of 10-crown-O_3 (**2O**) is 1.707 Å as listed in Table I. The same trend is seen in the Comp-X radius. Therefore, the macrocyclic amines have larger holes than the macrocyclic ethers with the same number of atoms (n) in the crown ring.

Figure 3 displays the space filling models of (9-crown-O_3)Li^+ (**1O**[Li^+]) and (12-crown-N_3)Li^+(**4N**[Li^+]) using the optimized structures. They have the smallest and the largest Comp-X radii of the *n*-crown-X_3, respectively. As the Comp-N radius for the cyclic amine (1.865 Å) is larger than that of the crown ether (1.541 Å), the Li^+ion in the amine complex lies 0.504 Å above the nitrogen plane and the cation in the ether complex lies 1.141 Å above the oxygen plane. Therefore, we can see a smaller part of the Li^+ ion in Figure 3b than in Figure 3a.

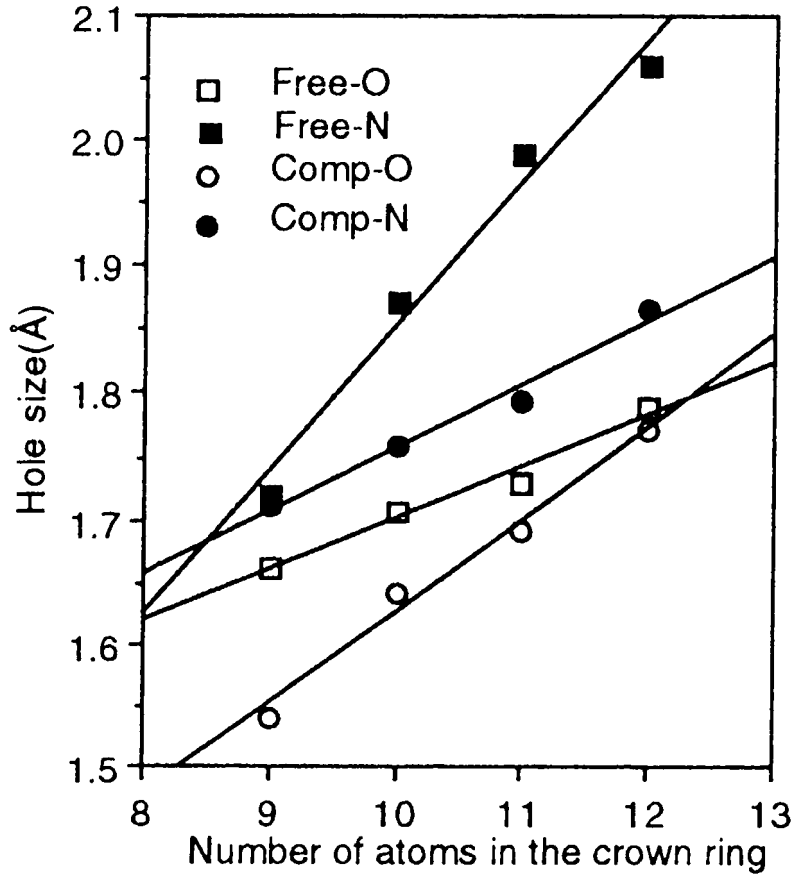

Figure 2. The change of the Free-X and Comp-X radii as a function of the number of atoms in the crown ring of *n*-crown-X_3 (C = O and N, *n* = 9, 10, 11 and 12) using the MNDO calculations.

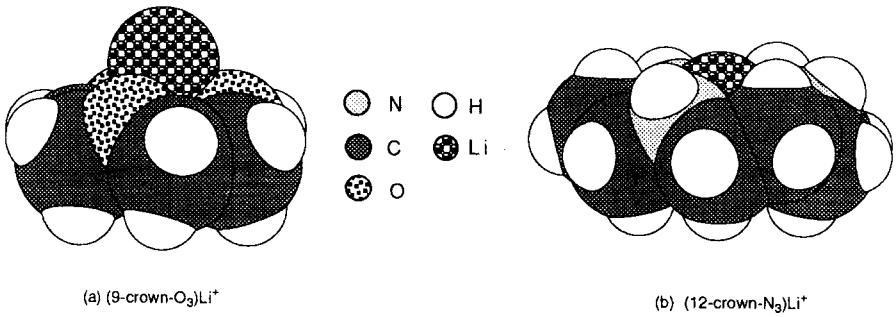

Figure 3. Space filling models of (9-crown-O_3)Li^+ (**1O**[Li^+]) and (12-crown-N_3)Li^+ (**4N**[Li^+]) by use of optimized coordinates of the MNDO calculations.

Table II. Stabilization energies (ΔE_{stab}), Free-O, Comp-O radii, and Li-O lengths of complexes with Li^+ and hole size of 12-crown-O_4 (**5**) with D_{2d} and C_{4v} symmetries[a]

Method	ΔE_{stab}	Free-O	Comp-O	Li-O
Symmetry: C_{4v}				
6-31G	99.3(81.8)[c]	1.830	1.769(1.776)[b]	1.862(1.959)[b]
MNDO	68.7(88.4)[c]	1.864	1.857	2.131
Symmetry: D_{2d}				
6-31G	114.4(98.8)[c]	2.050	1.827	1.827
MNDO[a]	54.6(100.9)[c]	2.040	1.968	1.968

[a] Energy in kcal mol^{-1} unit and length in Å unit.
[b] Values from (12-crown-4)Li(NCS) with C_{4v} symmetry.
[c] ΔE_{stab} from 6-31G*//6-31G and 6-31G*//MNDO calculations.

The Free-X lines for both X = O and N lie over the corresponding Comp-X lines. As listed in Table I, the estimated Free-O and Comp-O radii of 9-crown-O_3 (**1O**) were 1.661 and 1.541 Å, respectively. The difference of the two radii (Δr_{FC}) is 0.120 Å. Although 12-crown-O_3(**4O**) shrinks due to the complex formation with the Li^+ ion, its Δr_{FC} is only 0.018 Å. **1O** required a larger geometric change than **4O** in making the Li^+ complex. On the other hand, the Δr_{FC} of the Free-N and Comp-N radii is smallest in 9-crown-N_3 (**1N**) (0.007Å) and largest in 12-crown-N_3 **4N** (0.194 Å). Therefore, the holes of **4O** and **1N** are very suitable for the Li^+ ion. The hole of **1O** is too small and that of **4N** is too large to accommodate the Li^+ ion.

2.2. THE INTERACTION ENERGY BETWEEN A CROWN RING AND A CATION

Another factor determining the ion selectivity is the magnitude of stabilization energy due to complex formation. The D_{2d} and C_{4v} geometries of **5** and their Li^+ complexes were optimized by using *ab initio* MO calculations with the 6-31G basis set as well as the MNDO calculations. The results are listed in Table II.

The largest stabilization energy of 114.4 kcal mol^{-1} was calculated for the **5** [Li^+] complex with the D_{2d} symmetry. This value is larger by 12.5 (17.0) kcal mol^{-1} than that with the C_{4v} symmetry at the 6-31G//6-31G (6-31G*//6-31G) level of theory [16]. The calculations for 12-crown-X_3 also showed the stabilization energies to be smaller than those for the crown ethers with four donor atoms.

The solvation energy for the Li^+ ion is almost 120 kcal mol^{-1} [17]. It is necessary for crown compounds to release stabilization energies more than or equal to the solvation energy for the Li^+ ion in order to desolvate and make a complex with the cation. Therefore, four donor atoms in the 12-membered ring are not

sufficient to bind a Li^+ ion strongly even though they have suitable holes for the Li^+ ion. This is consistent with the experimental results that crown ethers with 12- or 13-membered rings do not make stable 1 : 1 complexes with the Li^+ ion [5].

2.3. THE EFFECT OF SIDE ARMS

Other building blocks to hand are side arms with several types of functional groups such as ether, amine, ester and so on [6]. A donor atom in a side arm can bind the Li^+ ion and release extra stabilization energy. This stabilization should reflect on the cation-binding property of crown compounds. 12-Crown-NO_3 (**6a**) , i.e., aza-12-crown-4, has a hydrogen atom which is substituted with one of these side arms, **b**–**h**. Li^+ complexes of **6b** and **6d** [18] whose amino-nitrogen or ether-oxygen atom on the side arm acts as the fifth binding donor for the Li^+ ion was optimized at the MNDO level. The 6-31G//MNDO level of theory demonstrated that the Li^+ complex of **6b** offers larger stabilization energy by 4.6 kcal mol^{-1} than that of **6d**. Therefore, theoretical results expect that **6a** with the amine arm may exhibit a selective binding and transporting of the Li^+ ion.

3. Experimental Characterization of Azacrown Ethers with a Side Arm [6]

3.1. Li^+ ION SPECIFIC LIQUID MEMBRANE TRANSPORT

According to theoretical considerations, the combination of a 12-membered ring with four donor atoms and an amine side arm is most likely to selectively bind and transport Li^+ ions. Therefore, we prepared a series of armed aza-12-crown-4 derivatives with side arms, **6b–6h**, from **6a**. They have amine- (**b** and **c**), ether- (**d**), ester- (**e**), amide (**f**), nitrile-(**g**) and pyridine (**h**) functionalized sidearms as the fifth cation-binding site. The transport of Li^+, Na^+ and K^+ ions across a CH_2Cl_2 liquid membrane was studied by using a U-tube glass cell (2.0 cm, i.d.) as described before [19]. The initial rates obtained under single and competitive transport conditions are summarized in Table III.

Introduction of a sidearm to the aza-12-crown-4 system greatly modified transport functionality, i.e., the rate of the single cation transport. In the case of **6d** and **6e** which have an ether and an ester arm, respectively, the side arm enhanced transport rates especially for Na^+ ions. **6g** with a nitrile-arm rarely mediated the cation transport. In contrast, **6b** and **6c** with an amine arm exhibited Li^+ ion selectivity which is not observed for the other aza-12-crown-4 derivatives. They selectively and efficiently transported Li^+ ions under competitive cation transport conditions as well [20]. The transport rate of a 14-crown-4 derivative (**8**) [21], which is known to be one of the best ionophores for the Li^+ ion, was measured in order to compare its activity as an ion carrier with the present armed crown ethers [22]. Since its Li^+ ion transport rate (1.9×10^7 mol h^{-1}) is less than 1/3 of those for **6b** and **6c**, the present aza-12-crown-4 derivatives with the amine arm showed an excellent transport functionality for the Li^+ ion.

Table III. Cation transport profiles of mono and double armed crown ethers and related carriers

Ether	Transport rate × 10^7 (mol h^{-1}) Li^+	Na^+	K^+
	[A] Single Cation Transport[a]		
6b	6.3	1.4	0.2
6c	8.5	1.2	0.5
6d	1.9	6.8	4.3
6e	0.6	4.9	2.8
6g	<0.2	0.4	<0.1
6i	0.3	0.6	0.4
8	1.9	0.3	<0.1
	[B] Competitive Cation Transport[a]		
6b	11.2	2.4	0.4
6c	19.2	3.5	0.8
6d	2.4	8.8	4.0
8	2.1	0.6	<0.1
	[B] Competitive Cation Transport[a]		
7b	95.8	7.7	0.4
7e	40.0	68.0	9.2
7f	9.2	10.2	0.3
7g	0.7	0.2	<0.1
7h	29.0	20.0	0.3
7i	1.3	<0.1	<0.1

[a] Conditions: [A] $MClO_4$ 0.50 mmol in H_2O 5 ml//Crown 0.0372 mmol in CH_2Cl_2 12 ml//H_2O 5 ml. [B] $LiClO_4$ 0.50 mmol, $NaClO_4$ 0.50 mmol, $KClO_4$ 0.50 mmol in H_2O 5 ml//Crown 0.0372 mmol in CH_2Cl_2 12 ml//H_2O 5 ml.

3.2. FAB MS BINDING EXPERIMENTS

The cation binding behaviors of the armed crown ethers were largely dependent on the type of sidearm. The FAB MS [23] competition technique was used to assess their binding ability for Li^+, Na^+, and K^+ ions on a semiquantitative level [24]. Table IV summarizes relative peak intensities of [ether + metal]$^+$ ions which reflect relative cation binding affinities. The relative peak intensities of the Li^+ ion for **6b** (100/20) and **6c** (100/24) are four or five times as large as those for the Na^+ ion. Values in parenthesis are ratios of relative peak intensities (Li^+/Na^+) for the two ions. Amine-functionalized sidearms enhanced binding selectivity for

Table IV. Cation binding selectivities of mono and double armed crown ethers assessed by FAB-MS

Ether	Relative peak intensity		
	Ether + Li^+	Ether + Na^+	Ether + K^+
Single armed derivatives[a]			
6a	100	57	20
6b	100	20	23
6c	100	24	11
6d	21	100	5
6e	12	100	2
6f	86	100	3
6g	100	55	7
6h	100	98	4
6i	100	25	4
9a	49	100	13
9c	83	100	5
9e	64	100	3
9h	51	100	4
Double armed derivatives[a]			
7b	100	3	<1
7e	100	55	0
7f	100	7	0
7g	100	14	23
7h	100	13	0

[a] Conditions: LiCl, 0.0083 mol/L; Nal, 0.0083 mol/L; Kl, 0.0083 mol/L; Iariat ether or double armed ether, 0.0033 mol/L; in *m*-nitrobenzyl alcohol.

the Li^+ ion since the ratio of **6a** is 100/57. In contrast, ether- (**6d** : 21/100) and ester- (**6e** : 12/100) armed aza-12-crown-4 derivatives showed Na^+ ion selectivity, while amide- (**6f** : 86/100) and pyridine- (**6h** : 100/98) armed derivatives did not discriminate between these cations. While some 12-crown-4 derivatives have been reported to form sandwich-type 2 : 1 complexes [5], no corresponding peak was recorded in the FAB MS spectra under the conditions we employed. Takahashi and his coworkers used the same technique and analyzed several lariat ether-Na^+, K^+ and Ca^{2+} complexes. They concluded, as we observed, that the presence of cation-ligating sidearms in lariat ethers suppressed formation of sandwich-type 2 : 1 complexes [25].

In order to evaluate the hole size effect on cation binding, aza-15-crown-5 derivatives **9a**, **9c**, **9e** and **9h** were also examined. The Li^+/Na^+ratios for these derivatives were observed to be 49/100, 83/100, 64/100 and 51/100, respectively.

Table V. Crown ether-induced changes in ^{7}Li and ^{23}Na NMR chemical shifts[a]

Ether	^{7}Li	Ether	^{7}Li	^{23}Na
6a	1.6	**7a**	2.2	7.4
6b	2.4	**7b**	2.5	8.4
6c	2.1	**7e**	2.7	9.2
6d	1.5	**7f**	2.6	10.8
6e	1.6	**7g**	1.3	3.4
6f	2.3	**7h**	3.4	15.2
6g	1.2	**7i**	1.9	6.9
6h	2.3			

[a] Conditions: mono or double armed crown ethers, 0.025 mmol; $LiClO_4$ or $NaClO_4$, 0.025 mmol in CD_3CN-CH_3CN (2/3) 0.5 mL. Positive is downfield shift.

All the relative values for the K^+ ion are less than 13. Since the peaks for the Na^+ complexes were larger than those for the Li^+ and the K^+ complexes, all the 15-membered crown ethers used here were confirmed to exhibit Na^+ ion selectivity. Therefore, the combination of an amine-functionalized sidearm and a 12-membered crown ring is essential for attaining Li^+ ion-specificity.

3.3. NMR CHEMICAL SHIFT EXPERIMENTS

Because the Li^+ ion is spherical and its chemical shift largely depends on its electron density, ^{7}Li NMR spectroscopy provides direct information concerning the interaction between the Li^+ ion and the donor atoms in a crown ring as well as a side arm [26]. Table V summarizes changes in the ^{7}Li NMR chemical shifts in the presence of several armed crown ethers. The ^{7}Li chemical shifts observed for crown ethers **6d**, **6e**, and **6g** with ether, ester, and nitrile arms ($\Delta\delta$ = 1.2–1.6 ppm) are almost the same as that for **6a** without a side arm ($\Delta\delta$ = 1.6 ppm). Therefore, their sidearms do not participate in forming the Li^+ complexes. On the other hand, **6b**, **6c**, **6f** and **6h**, which included amine, amide, and pyridine moieties on their sidearms, showed larger changes in ^{7}Li shifts ($\Delta\delta$ = 2.1–2.4 ppm) than that of **6a**. This result clearly indicates that the donor atoms on these sidearms effectively coordinate with the Li^+ ion trapped in their aza-12-crown-4 rings. The nature of the sidearm greatly influenced the Li^+ ion binding behavior.

^{13}C NMR spectroscopy provided further structural information on the armed crown ether-alkali metal complexes. Figure 4 shows the Li^+ and Na^+ induced changes in the chemical shifts for selected carbons of the crown ethers **6b** and

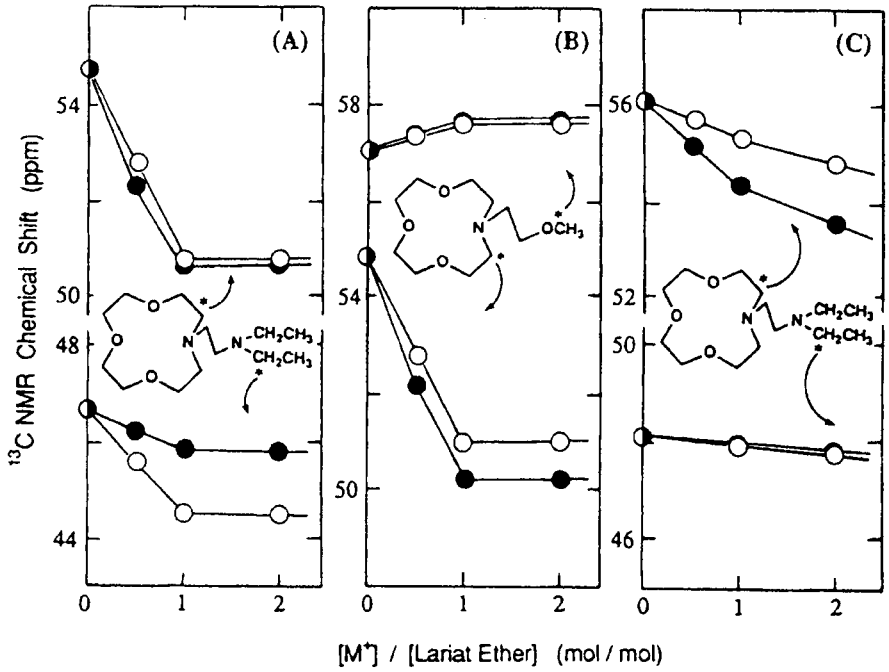

Figure 4. Li^+- and Na^+-induced changes in ^{13}C-NMR spectra of crown ethers **6b** and **6d**: (A) crown ether **6b** in CH_3CN/CD_3CN; (B) crown ether **6d** in CH_3CN/CD_3CN; (C) Lariat ether **6b** in CH_3OH/CD_3OD. ○: $M^+ = Li^+$, ●: $M^+ = Na^+$.

6d. When $LiClO_4$ salt was added to an acetonitrile solution of **6b**, significant and continuous shifts were observed for both crown ring and sidearm carbons (Figure 4A).

The titration curves for the ring carbons of **6b** have a sharp change in the presence of 1 equiv of the Li^+ ion, indicating that a 1 : 1 complex predominantly forms in the acetonitrile solution. Since the shifts of signals for the crown ring and the sidearm carbon were large ($\Delta\delta = -4.1$ ppm and -2.1 ppm), the amine-functionalized sidearm effectively coordinates with the Li^+ ion located in the aza-12-crown-4 ring. $NaClO_4$ salt induced somewhat different spectral changes of **6b** from the $LiClO_4$ induced ones. While the shifted value of the crown ring carbon ($\Delta\delta = -4.2$ ppm) is almost the same as that observed for the Li^+ ion, the signal for the sidearm carbon shifted only by -0.8 ppm. Thus, the amine-functionalized sidearm seemed to scarcely interact with the Na^+ ion. On the other hand, the Li^+-induced chemical shift of the sidearm carbon of **6d** (Figure 4B) was modest ($\Delta\delta = +0.5$ ppm) and similar to the Na^+ induced shift ($\Delta\delta = +0.6$ ppm). Since the signal of the crown ring carbon shifted greatly in the presence of the Li^+ or the Na^+ ion ($\Delta\delta = -3.9$ ppm and -4.6 ppm), the ether-functionalized sidearm was confirmed to coordinate very weakly with both ions.

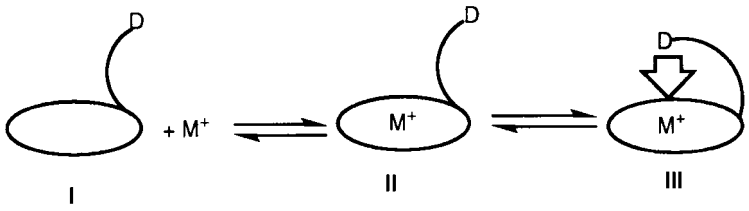

Drawing 2.

The nature of the solvent employed dramatically influenced the complex formation between an armed crown ether and a cation. As shown in Figure 4C, neither the sidearm carbon signal ($\Delta\delta < 0.1$ ppm) nor the crown ring carbon signal ($\Delta\delta < -1.2$ ppm) of **6b** shifted in a CH_3OH/CD_3OD solution. This probably indicates that even **6b** does not completely encapsulate the Li^+ and the Na^+ ions in such a polar medium as methanol.

The ^7Li and ^{13}C NMR spectroscopic studies suggested the role of the side arm was different in the complexes; the amine-functionalized crown ethers such as **6b** and **6c** use their side arms to encapsulate the Li^+ ion; the other arms in **6d–6h** do not participate in making complexes. The aza-12-crown-4 derivatives do not use their side arms in forming complexes with the Na^+ ion. According to these experimental results, we assumed the equilibrium among three types of coordination modes for the cation-crown system above (Drawing 2). M^+ and **I**, a free crown ether, first make a type **II** complex using four donor atoms in the crown ring but the side arm donor does not coordinate with the cation. After the formation of the type **II** complex, the armed crown ether completely holds the cation at its center by incorporating the side-arm donor and forming a type **III** complex. This conformation is suitable for the ion selective binding and transport. Hereafter, **I**, **II**, and **III** are designated as <[ ], <[M^+], and [>M^+], respectively, where "<" and "[ ]" indicate a side arm and an aza-12-crown-4 ring, respectively. Only **6b** and **6c** make type **III** complexes with a Li^+ ion and the type **II** complexes predominantly form in the other combinations of the side arms and cations.

4. Experimental Characterization of Double Armed Crown Ethers [27]

Double armed crown ethers may have a great advantage over single armed crown ethers as specific receptors because two arms work cooperatively to encapsulate an ion as shown in Figure 5. If this is correct, our approach is expected to improve both selectivity and efficiency in the Li^+ ion binding and transporting processes. The PM3 calculations of the Li^+ complex (**7b**[>Li^+<]) showed that the type B conformer is more stable than the type C conformer.

We systematically introduced various sidearms into **7a** to prepare a new series of Li^+ ion selective 'double armed' crown ethers which have amine- (**7b**), ester-

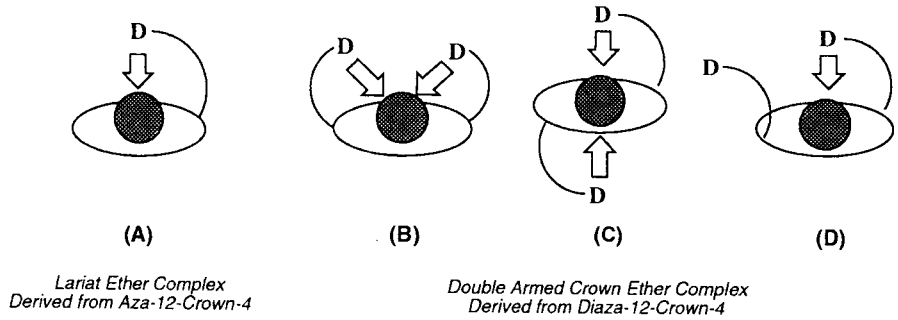

Figure 5. Coordination modes of double armed crown ethers.

(**7e**), amide- (**7f**), nitrile- (**7g**) and pyridine- (**7h**) arms. The sidearm effects on cation binding and transport properties were examined in a similar way for aza-12-crown-4 derivatives with one side arm.

FAB-MS studies revealed that double armed crown ethers selectively bound the Li^+ ion except for **7e** as listed in Table IV. $^7Li/^{23}Na$ NMR chemical shift experiments showed that the introduced double arms effectively acted in encapsulating both Li^+ and Na^+ ions. Although diaza-12-crown-4 derivatives displayed Li^+ ion selectivity in the binding process, most of them did not transport Li^+ ions selectively (Table III). Only the double armed crown ether **7b** having amine-functionalized sidearms attained Li^+ ion selectivity similar to the armed crown ether **6b**. It has to be emphasized that **7b** showed superior efficiency and selectivity in the Li^+ ion recognition process to **6b**, i.e., the cation transport rates are 95.8 and 11.2×10^7 mol h^{-1} for the Li^+ ion and 7.7 and 1.4×10^7 mol h^{-1} for the Na^+ ion, respectively. Moreover, the Li/Na ratio of **7b** is 12.4 which is almost three times as large as that for **6b** (4.7). Therefore, our strategy using the 'double armed crown ether' provided a promising possibility in design of a specific ionophore.

5. Theoretical Characterization Using Density Functional Calculations [28]

5.1. Density functional calculations without solvent effects

The experimental results suggested that the donor atom on the side arm did not always coordinate with the metal ion, i.e., the coordination depends on two factors, the kind of solvent and the combination of a cation and a donor atom on the side arm. The two factors should closely relate to the observed ion selectivity of **6b** and **6c**. In order to clarify why the aza-crown ethers with an amine arm have Li^+ ion selectivity, the density functional calculations with the DZVP basis sets were used. The DZVP sets were characterized as a double ζ basis set with polarization functions except for hydrogen atoms. The large basis sets were used for the present calculations since previous works indicated that neither the semi-empirical method nor *ab inito* MO calculations with low basis sets estimate proper

Table VI. The stabilization energies (kcal mol^{-1}) due to the complex formation with M^+ (M = Li, Na, and K) and aza-12-crown-4 with an amine or an ether side arm

Crown	Cation	ΔE_1	ΔE_2	ΔE_3
6b	Li^+	−90.9	−104.6	−13.8
	Na^+	−69.5	−79.6	−10.1
	K^+	−46.4	−54.6	−8.0
6d	Li^+	−88.2	−102.3	−14.0
	Na^+	−65.6	−78.8	−13.1
	K^+	−44.4	−54.3	−9.9

stabilization energies due to complex formation. We used the DGauss program [29] in Unichem on the Cray Y-MP2E computer at the Computer Science Department, Asahi Chemical Industry, Co. Ltd. and exchange-correlation energies were obtained by the Vosko-Wilk-Nusair method [30]. On this level auxiliary functional Al was used to calculate the exchange-correlation energy. The nonlocal corrections based on the Becke-Perder method [31] were performed perturbatively after geometry optimization.

In order to estimate the energy relationship among the free ligands, the types **II** and **III** complexes, we calculated the energies according to the following equations,

$$M^+ < [\,] \rightarrow < [M^+] \quad \Delta E_1 \tag{1}$$

$$M^+ < [\,] \rightarrow [> M^+] \quad \Delta E_2 \tag{2}$$

$$< [M^+] \rightarrow [> M^+] \quad \Delta E_3 \tag{3}$$

ΔE_1 and ΔE_2 are the stabilization energies due to complex formation by using four and five donor atoms, respectively. ΔE_3, which is defined as the difference between ΔE_1 and ΔE_2, is a measure for the ability of the side arm coordination to the metal ion. Table VI lists these energies for Li^+, Na^+ and K^+ complexes.

Due to the complex formation in the gas phase, the Li^+ ion releases the largest stabilization energies, the K^+ the smallest, and the Na^+ in-between as expected. For example, the ΔE_1 for **6b** are −90.9, −69.5 and −46.4 kcal mol^{-1} and ΔE_2 are −104.6, −79.6 and −54.6 kcal mol^{-1} for Li^+, Na^+ and K^+ complexes, respectively. ΔE_1 and ΔE_2 for the complexes with **4** and Li^+ are −88.2 and −102.3 kcal mol^{-1}, respectively. Although all the parent crown rings have one N and three O atoms, **6d** interacts with cations more weakly by ca. 2 kcal mol^{-1} than **6b**. In the Na^+ and K^+ complexes, both ΔE_1 and ΔE_2 for the amine arm are also larger by 0.3–3.9 kcal mol^{-1} than those for the ether arm.

It is important to point out that the oxygen donor on the side arm of **6d** binds alkali cations stronger than **6b** since all the ΔE_3 values for the ether arm are larger than those for the amine arm, i.e., ΔE_3 for **6b** and **6d** are -10.1 and -13.1 kcal mol^{-1} for the Na^+ complexes and -8.0 and -9.9 kcal mol^{-1} for the K^+ complexes, respectively. $\Delta\Delta E_3$, the energy difference between ΔE_3's of the **6b** and **6d** complexes, is 3.0 kcal mol^{-1} for the Na^+ ion and 1.9 kcal mol^{-1} for the K^+ ion. However, the $\Delta\Delta E_3$ is only 0.2 kcal mol^{-1} for the Li^+ ion.

As mentioned above, the experimental data suggested that in the acetonitrile solution only the Li^+ ion forms the type **III** complex with **6b** and the other combinations among the cations and the azacrown derivatives adopt only the type **II** geometries. However, ΔE_3 for the Li^+ ion is estimated to be more than 10 kcal mol^{-1}, and therefore, the type **III** complexes are more stable than the type **II** complexes in the gas phase. In Na^+ and K^+ complexes, we obtained similar results although the ΔE_3 values are smaller than those for the Li^+ complexes. These results are not consistent with the experimental data in the solution. The solvent effect probably explains the discrepancy of the results between the two phases.

5.2. Effect of solvation

According to the space filling drawings of **6b**$<[Li^+]$ and **6b**$[>Li^+]$ in Figure 6, it is very easy to find a space where solvents can access the central metal in the complex. That is, two or one solvent molecules can access the central metal, respectively. Therefore, we optimized model complexes in which two waters coordinate with the central metal ion in the type **II** complex, $<[M^+](OH_2)_2$, and one water in the type **III** complex, $[>M^+](OH_2)$ (M = Li and Na). The central metal cation contacts with one water for $[>Li^+](OH_2)$ or two for $<[Li^+](OH_2)_2$ within the sum of van der Waals radii as shown in Figure 6.

Six ligands coordinate with the cations in both complexes because the cation should have a similar coordination environment in order to compare the stabilization energies due to the complex formation. For the estimation of the solvation effect, we consider the following reactions,

$$M^+ + <[\,] + 2H_2O \rightarrow <[M^+](OH_2)_2 \qquad \Delta E_4 \tag{4}$$

$$M^+ + <[\,] + H_2O \rightarrow <[M^+](OH_2)_2 \qquad \Delta E_5 \tag{5}$$

$$<[M^+](OH_2)_2 \rightarrow [>M^+](OH_2) + H_2O \quad \Delta E_6 \tag{6}$$

and calculated the energies, ΔE_4 and ΔE_5, which are the stabilization energies released by the $<[M^+](OH_2)_2$ and $[>M^+](OH_2)$ complex formation, respectively. In Equation (6), the donor atom in the side-arm removes one solvent water and coordinates with the central metal (Drawing 3).

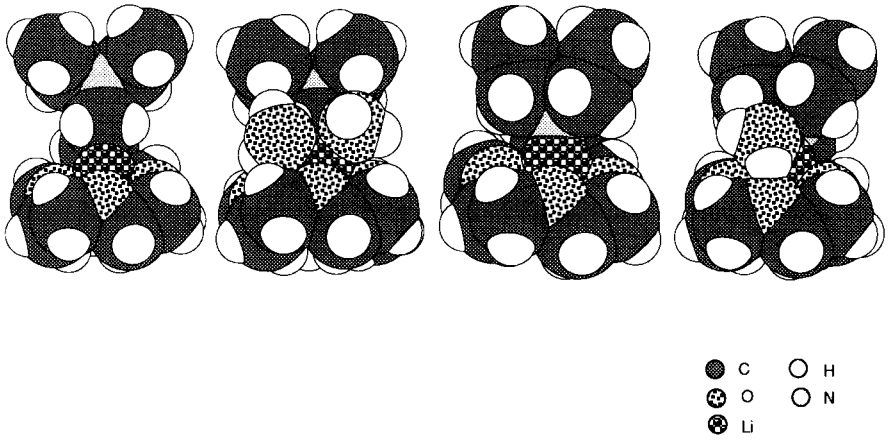

Figure 6. Space filling drawings of the optimized structures of the complexes of **6b** and Li^+ with and without H_2O as solvent.

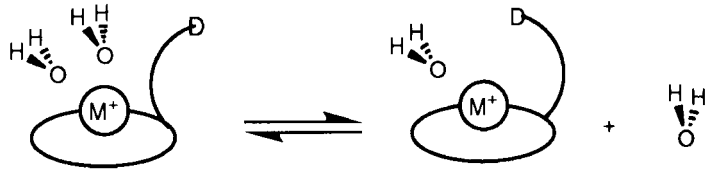

Drawing 3.

ΔE_6, which is defined as the difference between ΔE_4 and ΔE_5, is an index as to whether or not the side arm has an ability to replace the solvent as a ligand with its donor atom. If ΔE_6 is positive, the first case, the side-arm donor cannot remove a solvent and a complex such as $[>M^+](OH_2)$ will not form in the solution. If ΔE_6 is almost equal to 0.0 (the second case), there should be equilibration between the type **II** and **III** complexes. On the other hand, the negative value, the third case, means that aza-12-crown-4 with the amine arm can completely encapsulate the cation in its cavity. Therefore, ΔE_6 should be around 0.0 or negative for the crown molecules which can transport Li^+ selectively. Table VII summarizes the calculated energies for Li^+ and Na^+ complexes of **6b** and **6d**.

It is remarkable that ΔE_4 for **6b** $< [Li^+](OH_2)_2$ is almost equal to ΔE_5 for **6b**$[>Li^+](OH_2)$, and then, ΔE_6 is only -0.1 kcal mol^{-1}, the second case. In this complex, we have the combination of the amine arm and the Li^+ ion. **6b** was observed to transport the Li^+ ion selectively. On the other hand, ΔE_5 and ΔE_6 for the Na^+ ion turned out to be -91.6 and -87.9 kcal mol^{-1} so that ΔE_6 is estimated to be 3.7 kcal mol^{-1}. The positive value, the first case, means that we cannot expect selective Na^+ ion transport by **6b**. This is what was observed. Therefore, the theoretical expectations are consistent with the experimental results.

In the case of the combination of **6d** and the Li^+ ion, ΔE_4 and ΔE_5 were calculated to be -112.1 and -108.8 kcal mol^{-1} for the Li^+ complexes and -91.7

Table VII. The stabilization energies (kcal mol^{-1}) due to the complex formation with M^+ (M = Li and Na) and the armed aza-12-crown-4 with the solvent effect

Crown	Cation	ΔE_4	ΔE_5	ΔE_6
6b	Li^+	−111.9	−112.0	−0.1
	Na^+	−91.6	−87.9	3.7
6d	Li^+	−112.1	−108.8	3.3
	Na^+	−91.7	−88.4	3.3

and −88.4 kcal mol^{-1} for the Na^+ complexes, respectively. Replacing one OH_2 ligand and the coordination of the ether donor result in the loss of stability of the complex although its ΔE_6 value is as small as 3.3 kcal mol^{-1}. The same value was obtained for the Na^+ complex. Therefore, neither the Li^+ nor the Na^+ ion can make the type **III** complex with **6d** in the acetonitrile solution. They only form the type **II** complex which is not suitable for selective inclusion and effective transport of the cations. This is also what we observed in solution.

6. Concluding Remarks

Our strategy for designing new receptor molecules specific for the Li^+ ion is to combine the two methods, theoretical calculations and the experimental technique. The calculations can estimate many properties which are required for receptor molecules before their synthesis. The experimental work can characterize their properties and obtain information which theoretical calculations do not give. After characterization of new molecules in terms of experimental technique, we use theoretical calculations again in order to explain experimental results.

The other key to our strategy is to use building blocks which are suitable for constructing new receptor molecules. In developing the Li^+ ion-specific receptors, we just used two types of blocks, i.e., an aza-12-membered crown ring and side arms with a functional group. It is possible to synthesize a variety of crown ether derivatives by just changing a functional group on the side arm.

The present strategy worked well for the purpose of synthesizing new molecules which selectively bind and transport the Li^+ ion as mentioned above. The aza-12-crown-4 derivatives with one and two amine arms, i.e., **6b** and **7b**, shows the desired property. We need further improvement of our molecules since these molecules cannot exhibit their ability in polar solvents such as methanol. We are now extending investigations to design and develop new molecules of further desired properties [32].

Acknowledgements

This work was supported in part by a Grant-in-Aid for Scientific Research (No. 08454205) from the Ministry of Education, Sports and Culture, Japan. The authors thank the Computer Center, Institute for Molecular Science at the Okazaki National Research Institutes for the use of the HITAC M-600 and S-820/80 computers and the Library Program GAUSSIAN 90.

References

1. (a) C.J. Pedersen: *J. Am. Chem. Soc.* **89**, 7017 (1967). (b) D.J. Cram: *Angew. Chem., Int. Ed. Engl*. **27**, 1009 (1988). (c) J.M. Lehn: *Angew. Chem., Int. Ed. Engl*. **27**, 90 (1988).
2. (a) P.G. Potvin and J.M. Lehn: In *Synthesis of Macrocycles* (Eds. R.M. Izatt and J.J. Christensen), Vol 3, John-Wiley & Sons, New York, p. 167 (1987). (b) H. Tsukube: In *Liquid Membranes*: Chemical Applications (Eds. T. Araki and H. Tsukube), CRC Press, Florida, 51 (1990). (c) H. Tsukube: *Coord. Chem. Rev.* **148**, 1 (1996).
3. (a) K. Kimura, T. Yamashita, M. Kaneshige, and M. Yokoyama: *J. Chem. Soc. Chem. Commun.* 969 (1992). (b) Y. Habata, M. Ikeda, and S. Akabori: *Tetrahedron Lett.* **33**, 3157 (1992). (b) K. Kobiro, Y. Tobe, K. Watanabe, H. Yamada, and K. Suzuki: *Anal. Lett.* **26**, 49 (1993). (c) W. Zazulak, E. Chapoteau, B. P. Czech, and A. Kumar: *J. Org. Chem.* **57**, 6720 (1992). (d) Z. Chen, O.F. Schall, M. Alcala, Y. Li, G.W. Gokel, and L. Echegoyen: *J. Am. Chem. Soc.* **114**, 444 (1992).
4. R.M. Izatt, K. Pawlak, J.S. Bradshaw, and R. Bruening: *Chem. Rev*. **91**, 1721 (1991).
5. (a) M.J. Calverley and J. Dale: *Acta Chem. Scand*. **B36**, 241 (1982). (b) B.D. White, K.A. Anrold, R.L. Garrell, F.R. Fronczek, R.D. Gandour, and G.W. Gokel: *J. Org. Chem.* **52**, 1128 (1987).
6. (a) H. Tsukube, K. Hori, and T. Inoue: *Tetrahedron Lett*. **34**, 6749 (1993). (b) H. Tsukube, T. Inoue, and K. Hori: *J. Org. Chem.* **59**, 8047 (1994).
7. Reviews: (a) E. Weber: In *Crown Ether and Analogues*. John Wiley & Sons: Chichester, p. 305 (1989). (b) L.F. Lindoy: In *The Chemistry of Macrocyclic Ligand Complexes*. Cambridge University Press: Cambridge, p. 103 (1989). (c) K.E. Krakowiak, J.S. Bradshaw, D.J. Zamecka-Krakowiak, and R.M. Izatt: *Chem. Rev.* **89**, 929 (1989). (d) G.W. Gockel, and J.E. Trafton: In *Cation Binding by Macrocycles*, Marcel Dekker: New York, p. 253 (1990).
8. (a) T. Yamabe, K. Hori, K. Akagi, and K. Fukui: *Tetrahedron* **35**, 1065 (1979). (b) K. Hori, H. Yamada, and T. Yamabe: *Tetrahedron* **39**, 67 (1983). (c) E.T. Seidl, and H. F. Schaefer III: *J. Phys. Chem.* **95**, 3589 (1991). (d) E.D. Glendening, D. Feller, and M.A. Thompson: *J. Am. Chem. Soc.* **116**, 10657 (1994).
9. Y.L. Ha and A.K. Chakraborty: *J. Phys. Chem.* **96**, 6410 (1992).
10. (a) M.J. Bovill, D.J. Chadwick, I.O. Southerland, and D. Watkin: *J. Chem. Soc., Perkin Trans. 2* 1529 (1980). (b) G. Wipff, P. Weiner, and P.A. Kollman: *J. Am. Chem. Soc.* **104**, 3249 (1982). (c) M.G.B. Drew, D.G. Nicholson: *J. Chem. Soc., Dalton Trans*. **1986**, 1543. (d) W.L. Hase, M.-C. Richou, and S.L. Mondro: *J. Phys. Chem.* **93**, 539 (1989).
11. (a) A.E. Haward, U.C. Singh, M. Billeter, and P.A. Kollman: *J. Am. Chem. Soc*. **110**, 6984 (1988). (b) L.X. Dang and P.A. Kollman: *J. Am. Chem. Soc.* **112**, 5716 (1990). (c) Y. Sun and P.A. Kollman: *J. Chem. Phys.* **97**, 5108 (1992). (d) J. van Eerden, S. Harkema, and D. Feil: *J. Phys. Chem.* **92**, 5076 (1988). (e) T.P. Straatsma and J.A. McCammon: *J. Chem. Phys.* **91**, 3631 (1989). (f) F.T.H. Leuwerink, S. Herkema, W.J. Briels, and D. Feil: *J. Compt. Chem.* **14**, 899 (1993). (g) L. Troxler and G. Wipff: *J. Am. Chem. Soc*. **116**, 1468 (1994).

12. (a) G. Ranghino, S. Romano, J.M. Lehn, and G. Wipff: *J. Am. Chem. Soc.* **107**, 7873 (1985). (b) Y. Ha and A.K. Chakraborty: *J. Phys. Chem.* **95**, 10781 (1991). (c) Y. Ha and A.K. Chakraborty: *J. Phys. Chem.* **97**, 11291 (1993).
13. K. Hori, H. Tsukube, and T. Inoue: *Tetrahedron* **49**, 3959 (1993).
14. MOPAC ver.5, J.J.P. Stewart: QCPE # 455.
15. Gaussian 90, Revision F, Frisch, M.J. Head-Gordon, G.M. Trucks, W. Foresman, J.B. Schlegel, H.B. Raghavachari, K. Robb, W. Binkley, J.S. Gonzalez, C. Defrees, D.J. Fox, D.J. Whiteside, R.A. Seeger, R. Melius, C.F. Baker, J. Martin, R.L. Kahn, L.R. Stewart, J.J.P. Topiol, S., and J.A. Pople: Gaussian Inc., Pittsburgh PA (1990).
16. The values in parenthesis are energies at the 6-31G*//6-31G level of theory.
17. *Kagaku Binran*, 3rd Ed., Maruzen (1984).
18. The calculation used the $CH_2CH_2NH_2$ arm instead of the $CH_2CH_2N(C_2H_5)_2$ arm.
19. H. Tsukube, H. Adachi, and S. Morosawa, *J. Org. Chem*. **56**, 7102 (1991).
20. Larger transport rates were observed under competitive cation transport conditions than those under single cation transport conditions. High concentration of ClO_4^- anion may accelerate cation transport rate.
21. Liquid-liquid extraction experiments revealed that transport selectivity depended on the uptake behavior of metal cation into the CH_2Cl_2 membrane phase.
22. K. Kimura, H. Oishi, T. Miura, and T. Shono: *Anal. Chem.* **59**, 2331 (1987).
23. (a) R.A.W. Johnstone and M.E. Rose: *J. Chem. Soc. Chem. Commun.* 1268 (1983). (b) G. Bonas, C. Bosso, and M.R. Vignon: *Rapid Commun. Mass Spectrom*. **2**, 88–89 (1989).
24. (a) I. Stibor, P. Holy, J. Závada, J. Koudelka, J. Novák, J. Zajicek, and M. Belohradsky: *J. Chem. Soc., Chem. Commun.* 1581 (1990). (b) H. Tsukube: In *Comprehensive Supramolecular Chemistry* Pergamon Press, Oxford, **8**, p. 425 (1996).
25. T. Takahashi, A. Uchiyama, K. Yamada, B.C. Lynn, and G. Gokel: *Supramol. Chem.* **2**, 177 (1993).
26. K. Kimura, T. Yamashita, and M. Yokoyama: *J. Chem. Soc., Perkin Trans. 2* 613 (1992).
27. H. Tsukube, S. Shinoda, Y. Mizutani, M. Okano, K. Takagi, and K. Hori: *Tetrahedron* **53**, 3487 (1997).
28. K. Hori, T. Inoue, and H. Tsukube: *Tetrahedron* **52**, 8199 (1996).
29. J. Anzelm and E. Wimmer: *J. Chem. Phys.* **96**, 1280 (1992).
30. S.H. Vosko, L. Wilk, and M. Nusair: *Can. J. Chem.* **58**, 1200 (1980).
31. (a) A.D. Beck: *Phys. Rev. A* **38**, 3098 (1988). (b) A.D. Becke: *J. Chem. Phys.* **84**, 4524 (1986). (c) J.P. Perdew: *Phys. Rev. B* **33**, 8822 (1986).
32. H. Tsukube, Y. Mizutani, S. Shinoda, M. Tadokoro, and K. Hori: *Tetrahedron Lett.* **38**, 5021 (1997).